Trajectory Design considering Derivative of Jerk for Head-positioning of Disk Drive System with Mechanical Vibration

Byung-hoon Chang and Yoichi Hori

Rm. Ce-503, Institute of Industrial Science, University of Tokyo,
4-6-1 Komaba, Meguro, Tokyo, 153-8505, JAPAN
Tel: +81-3-5452-6289, Fax.: +81-3-5452-6288
E-mail: chang@horilab.iis.u-tokyo.ac.jp, hori@horilab.iis.u-tokyo.ac.jp

Abstract: In this paper, we propose a novel design method of target trajectory for high-speed and high-precision head-positioning of hard disk drive system. To realize smooth acceleration and deceleration, the derivative of jerk is considered not to activate any mechanical vibrations. We applied the well-known optimal control theory to fix the initial and terminal conditions. Moreover, we showed that various performance can be improved by introducing time varying weighting coefficients. Some experimental results using a 2.5 inch hard disk drive are shown to verify the effectiveness of the proposed method.

Key words: Hard Disk Drive, Target Trajectory, TDOF Control, Mechanical Vibration Suppression, Optimal Control

1 Introduction

Unlike semiconductor memory, Hard Disk Drive (HDD) requires quick and precise mechanical operation of the head known as head-positioning for write-in and read-out of data.

In this positioning control of HDD system, three kinds of servo control methods have been commonly applied, namely, seek mode, settling mode and following mode. In the seek mode, the head is driven from the current track close to the desired data track. In the settling mode, it is positioned on the center of the desired track. In the following mode, the head position should be kept within a certain area to read and write the data[1].

However, in this mode-switching type control system, residual vibration at mode-switch is a serious problem. To solve this problem, some techniques such as initial value compensation of controller's state variables have been proposed but they are complicated[2].

On the other hand, Two - Degrees - Of - Freedom (TDOF) controller does not need any mode-switching and the problems caused by switching do not exist[3][4]. In this method, a smooth target trajectory design not to excite any mechanical vibration is the most important problem.

The novel design method we propose in this paper aims at shortening seek time and minimizing jerk (rate of change of acceleration) which causes vibration. A novel cost function for minimizing jerk are firstly introduced, and the target trajectory is generated based on the well known optimal control theory with fixed initial and terminal conditions.

2 Trajectory design considering derivative of jerk

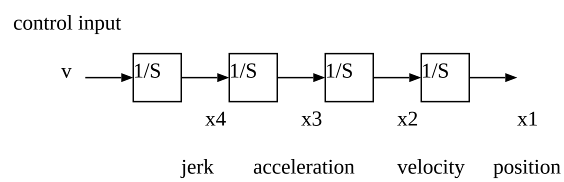

Figure 1: Simple model of VCM

First, the Voice Coil Motor (VCM) is simply modeled as shown in Fig.1. The state equations take the form of (1), where, x_1, x_2, x_3 and x_4 are position, velocity, acceleration, and jerk, respectively.

$$\begin{bmatrix} \dot{x_1} \\ \dot{x_2} \\ \dot{x_3} \\ \dot{x_4} \end{bmatrix} = \begin{bmatrix} 0 & 1 & 0 & 0 \\ 0 & 0 & 1 & 0 \\ 0 & 0 & 0 & 1 \\ 0 & 0 & 0 & 0 \end{bmatrix} \begin{bmatrix} x_1 \\ x_2 \\ x_3 \\ x_4 \end{bmatrix} + \begin{bmatrix} 0 \\ 0 \\ 0 \\ 1 \end{bmatrix} v \qquad (1)$$

Note that the jerk, x_4, is included as the new state variable. The cost function to be minimized is given by (2).

$$\begin{aligned} J &= \frac{1}{2}\int_0^{t_f} [\boldsymbol{x}^T(t)\boldsymbol{Q}\boldsymbol{x}(t) + \boldsymbol{v}^T(t)\boldsymbol{R}\boldsymbol{v}(t)]dt \\ &\quad + \frac{1}{2}\boldsymbol{x}^T(t_f)\boldsymbol{S}\boldsymbol{x}(t_f) \end{aligned} \qquad (2)$$

The integral of square of jerk derivative is also included in $v^T(t)Rv(t)$ together with position, velocity, acceleration, and jerk.

Boundary conditions are given by (3), where, t_f and a represent the access time and the access distance, respectively.

$$\boldsymbol{x}(0) \quad = \quad \begin{bmatrix} a \\ 0 \\ 0 \\ 0 \end{bmatrix}, \boldsymbol{x}(t_f) = \begin{bmatrix} 0 \\ 0 \\ 0 \\ 0 \end{bmatrix} \tag{3}$$

The Hamiltonian is given by (4).

$$H = \frac{1}{2}(\boldsymbol{x}^T(t)\boldsymbol{Q}\boldsymbol{x}(t)+\boldsymbol{v}^T(t)\boldsymbol{R}\boldsymbol{v}(t))+\boldsymbol{\lambda}^T(\boldsymbol{A}\boldsymbol{x}(t)+\boldsymbol{B}\boldsymbol{v}(\boldsymbol{t})) \tag{4}$$

The canonical equations are shown by (5) and (6), and here, x and λ vary according to these linear differential equations.

$$\dot{\boldsymbol{x}} \quad = \quad \frac{\partial H}{\partial \boldsymbol{\lambda}} = \boldsymbol{A}\boldsymbol{x} + \boldsymbol{B}\boldsymbol{v} \tag{5}$$

$$\dot{\boldsymbol{\lambda}} \quad = \quad -\frac{\partial H}{\partial x} = -\boldsymbol{Q}\boldsymbol{x} - A^T\boldsymbol{\lambda} \tag{6}$$

The optimal control input becomes:

$$\boldsymbol{v} \quad = \quad -\boldsymbol{R}^{-1}\boldsymbol{B}^T\boldsymbol{\lambda} \quad (\frac{\partial H}{\partial v} = \boldsymbol{R}\boldsymbol{v} + \boldsymbol{B}^T\boldsymbol{\lambda} = 0) \tag{7}$$

Using this optimal control input, the above-metioned canonical equations can be simplified to (8).

$$\begin{bmatrix} \dot{\boldsymbol{x}} \\ \dot{\boldsymbol{\lambda}} \end{bmatrix} = \begin{bmatrix} \boldsymbol{A} & -\boldsymbol{B}\boldsymbol{R}^{-1}\boldsymbol{B}^T \\ -\boldsymbol{Q} & -\boldsymbol{A}^T \end{bmatrix} \begin{bmatrix} \boldsymbol{x} \\ \boldsymbol{\lambda} \end{bmatrix} \tag{8}$$

From the transversality condition in the free terminal value case, (9) is obtained.

$$\boldsymbol{\lambda}(t_f) \quad = \quad \boldsymbol{S}\boldsymbol{x}(t_f) \tag{9}$$

As is well-known, by using assumption (10), the two point boundary value problem can be changed to a one point boundary value problem.

$$\boldsymbol{\lambda}(t) \quad = \quad \boldsymbol{P}(t_f - t)\boldsymbol{x}(t) \tag{10}$$

The Ricatti differential equation as shown in (11) is obtained from (8) and (10), where, $\tau = t_f - t$.

$$\dot{\boldsymbol{P}}(\tau) = \boldsymbol{P}(\tau)\boldsymbol{A} + \boldsymbol{A}^T\boldsymbol{P}(\tau) - \boldsymbol{P}(\tau)\boldsymbol{B}\boldsymbol{R}^{-1}\boldsymbol{B}^T\boldsymbol{P}(\tau) + \boldsymbol{Q} \tag{11}$$

The boundary condition $P(0) = S$ is derived from $\boldsymbol{\lambda}(t_f) = \boldsymbol{S}\boldsymbol{x}(t_f) = \boldsymbol{P}(t_f - t_f)\boldsymbol{x}(t_f) = \boldsymbol{P}(0)\boldsymbol{x}(t_f)$.

Here, the value $\boldsymbol{S} = \boldsymbol{P}(0) = \infty$ is substituted in order to fix the terminal value (x_f) precisely for HDD positioning control.

This is impossible in practice, therefore, by using the relation of $\boldsymbol{P}\boldsymbol{P}^{-1} = \boldsymbol{I}$, the Ricatti differential equation in terms of $\boldsymbol{P}^{-1}$ can be obtained as (12).

$$\begin{aligned} \dot{\boldsymbol{P}}^{-1}(\tau) \quad = \quad & -\boldsymbol{A}\boldsymbol{P}^{-1}(\tau) - \boldsymbol{P}^{-1}(\tau)\boldsymbol{A}^T + \boldsymbol{B}\boldsymbol{R}^{-1}\boldsymbol{B}^T \\ & - \boldsymbol{P}^{-1}(\tau)\boldsymbol{Q}\boldsymbol{P}^{-1}(\tau) \end{aligned} \tag{12}$$

This Ricatti equation can be solved starting from its initial condition $\boldsymbol{P}^{-1}(0) = 0$. Based on this solution, the differential equation (13) can be obtained from (8) and (10).

$$\dot{\boldsymbol{x}}(t) \quad = \quad (\boldsymbol{A} - \boldsymbol{B}\boldsymbol{R}^{-1}\boldsymbol{B}^T\boldsymbol{P}(\tau))\boldsymbol{x}(t) \tag{13}$$

Finally, the target trajectory $\boldsymbol{x}(t)$ can be generated by solving this differential equation (13).

3 Example of trajectory generation

3.1 Trajectory change in case of time-invariant weighting factor Q

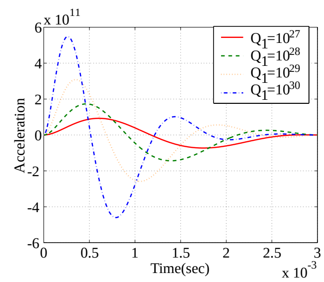

(a) Changes in q_1 $(q_2 = q_3 = q_4 = 0)$

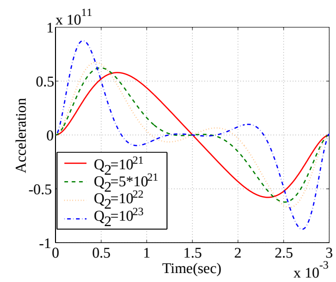

(b) Changes in q_2 $(q_1 = q_3 = q_4 = 0)$

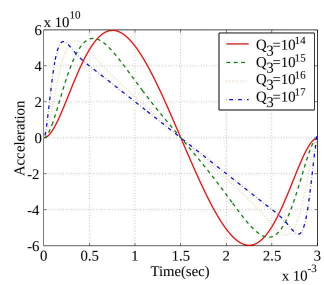

(c) Changes in q_3 $(q_1 = q_2 = q_4 = 0)$

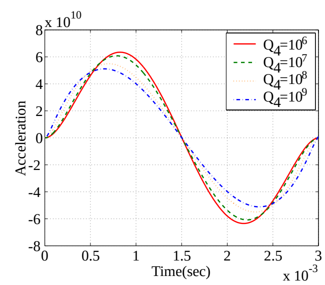

(d) Changes in q_4 $(q_1 = q_2 = q_3 = 0)$

Figure 2: Acceleration of obtained trajectories with changes in Q

Numerical computation is performed using MATLAB, where, the weighting factor Q appears as (14).

$$\boldsymbol{Q} = \begin{bmatrix} q_1 & 0 & 0 & 0 \\ 0 & q_2 & 0 & 0 \\ 0 & 0 & q_3 & 0 \\ 0 & 0 & 0 & q_4 \end{bmatrix}, \boldsymbol{R} = 1 \tag{14}$$

In this section, we explain the acceleration of obtained trajectories with changes in Q in terms of high-speed and high-precision.

Fig.2 shows the acceleration of obtained trajectories with changes in Q. In Fig.2 (a), we can see that the trajectory with changes in q_1, where $q_2 = q_3 = q_4 = 0$, has an asymmetric form. And we also can see that the response to positioning becomes quick as the value of the weighting factor q_1 becomes large. In this figure, we can check the response to positioning is the highest-speed around $q_1 = 10^{30}$.

However,it is not desirable as a target trajectory as any case with changes in q_1 causes overshoot.

In Fig.2 (b), (c), (d), we can see that the trajectory with changes in q_2, q_3, q_4 has a symmetric form. And we also can see that the jerk at the start and end become large, on the other hand, the jerk around the middle become small. However, large jerks at the ending points are not desirable as they cause mechanical vibrations.

From these considerations, we can find that the case when $Q = 0$ gives the most suitable target trajectory which induces the least vibration in these cases of time-invariant weighting factor Q.

Much higher speed positioning control system can be realized considering time-varying weighting for $Q(t)$.

3.2 Analytical solution where $Q = 0$

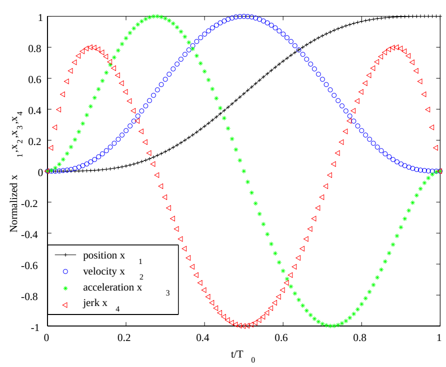

Figure 3: Normalized trajectory based on the equation (15) $\sim$ (18)

Even in the special case where $Q = 0$, it is also expected that jerk will be suppressed because jerk derivative is still included in the cost function. This concept is the same as the well-known SMART, but SMART only considered jerk. Like SMART theory, the mathmetical expression of our trajectory can be given by (15) $\sim$ (18), where $Q = 0$.

$$\begin{aligned} x_1(t) &= -20a(\frac{t}{T_0})^7 + 70a(\frac{t}{T_0})^6 \\ &\quad - 84a(\frac{t}{T_0})^5 + 35a(\frac{t}{T_0})^4 \qquad (15) \\ x_2(t) &= \frac{a}{T_0}[-140(\frac{t}{T_0})^6 + 420(\frac{t}{T_0})^5 \\ &\quad - 420(\frac{t}{T_0})^4 + 140(\frac{t}{T_0})^3] \qquad (16) \\ x_3(t) &= \frac{a}{(T_0)^2}[-840(\frac{t}{T_0})^5 + 2100(\frac{t}{T_0})^4 \\ &\quad - 1680(\frac{t}{T_0})^3 + 420(\frac{t}{T_0})^2] \qquad (17) \\ x_4(t) &= \frac{a}{(T_0)^3}[-4200(\frac{t}{T_0})^4 + 8400(\frac{t}{T_0})^3 \\ &\quad - 5040(\frac{t}{T_0})^2 + 840\frac{t}{T_0}] \qquad (18) \end{aligned}$$

Normalized trajectory of each state relevant to (15) $\sim$ (18) is shown in Fig.3. We can see from Fig.3 that jerks at the starting and ending points are suppressed effectively.

3.3 Trajectory in case of time-varying weighting for $Q(t)$

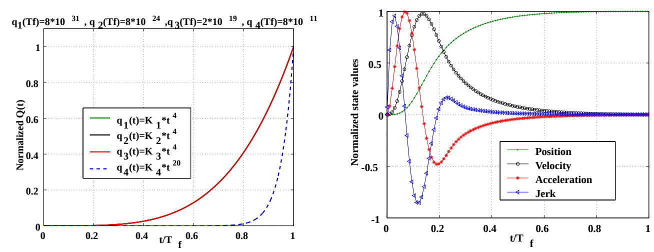

(a) Q(t) (b) Target trajectory

Figure 4: Trajectory for higher-speed seeking by $Q(t)$

For higher-speed seeking, we propose a trajectory which accelerates quickly at the start, decelerates slowly at the end, and positions smoothly at the end point. Such an asymmetric trajectory can be realized easily by using the time-varying weighting factor $Q(t)$ in our proposed method.

In this section, we introduce the target trajectory for higher-speed seeking which is generated based on the result of Section 3.1.

Some conditions for higher-speed trajetory is as follows:

- move to target position at high speed
- do not activate any overshoot
- keep smooth the velocity trajectory from the point in time of the maximum speed to the end
- minimize the jerk at the end

- must not exceed the maximum current

Finally, meeting the above conditions, we weight $Q(t)$ and design the trajectory for higher-speed seeking as shown in Fig.4.

4 Application to Hard Disk Drive(simulation)

Simulations were performed to verify the effectiveness of the proposed method. In the simulations, we applied the trajectory by $Q(t)$ mentioned in section 3.3 to an accurate system model of HDD. The model is that of a 2.5 inch HDD and is identical to that used by TOSHIBA Co. Ltd. in HDD research and development. The model includes features such as mechanical vibrations. In this section, the configuration of the simulation system is explained and simulation results are shown.

4.1 Reference method to be compared

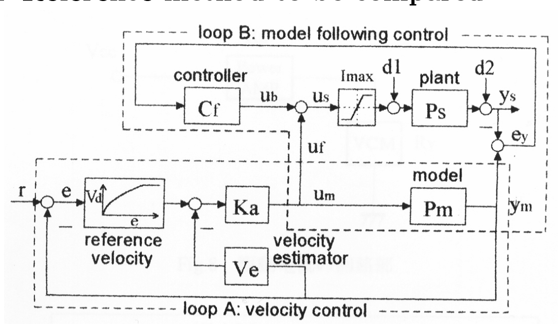

Figure 5: Model Following Control system

HDD seek control system based on Model Following Control (MFC) is shown in Fig.5. The control input in this case is a Bang-bang like waveform.

The trajectory is generated according to the remaining distance to the target track. It starts up with the bang-bang waveform for high-speed seeking. However, near the desired track, the trajectory slows down smoothly. We use this MFC system as the reference method to evaluate the proposed method.

4.2 Configuration of simulation system

The ideal block diagram of the proposed design method is shown in Fig.6.

Fig.6 shows the structure of TDOF control system. It is common to use the inverse system of the plant as the feedforward controller. However, when an unstable zero exists in the plant like in our case, the feedforward controller becomes unstable.

By taking advantage of the fact that we can generate all state variables' trajectories in our method, Taylor expansion is applied to calculate the coefficients for acceleration and jerk as shown in (19). This is used as

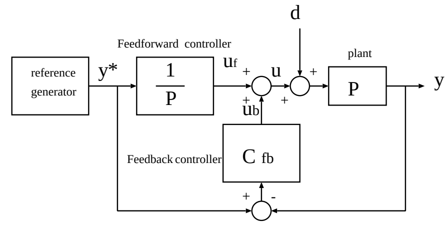

Figure 6: Ideal block diagram

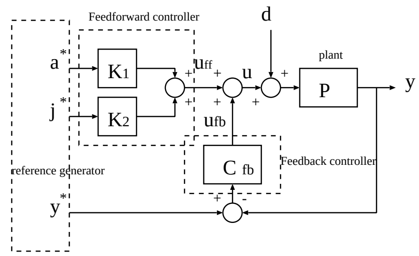

Figure 7: Reconstructed positioning control system

the feedforward controller as shown in Fig.7.

$$\frac{1}{P}y^* = K_1 s^2 y^* + K_2 s^3 y^* = K_1 a^* + K_2 j^* \qquad (19)$$

4.3 Simulation results

Simulations based on Fig.7 were carried out, where the number of access tracks are 1, 10 and 100 and access times are 1.2 [ms](1 track), 2.4 [ms](10 tracks) and 3.2 [ms](100 tracks).

Figs.8,9 and 10 show simulation results of the proposed method compared to the MFC trajectory.

From these figures, we can compare the time response and robustness of the proposed method to those of MFC. It is apparent that the proposed method shows quicker positioning performance than MFC method if there is no plant variation.

Here, the head positioning time is defined by the time taken before the head is positioned within ±10% of one track width.

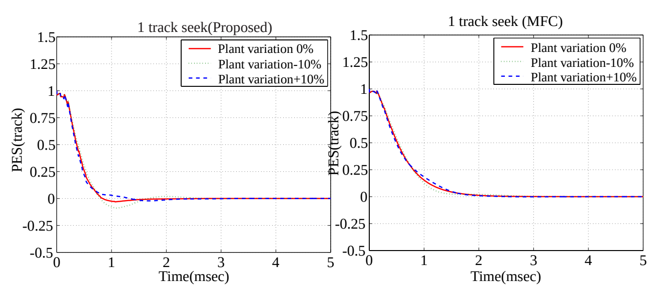

(a) Proposed (b) MFC

Figure 8: 1 track seek (simulation)

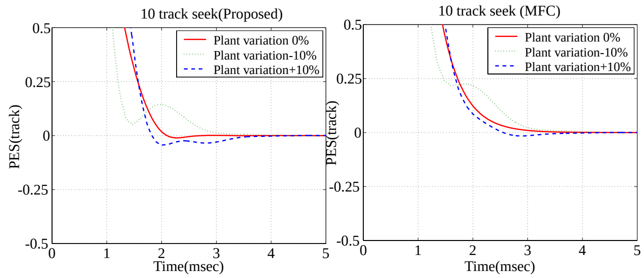

(a) Proposed (b) MFC

Figure 9: 10 track seek (simulation)

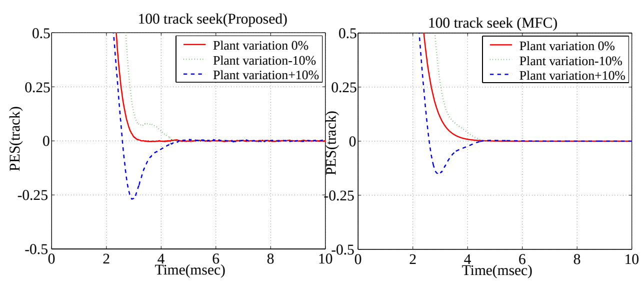

(a) Proposed (b) MFC

Figure 10: 100 track seek (simulation)

Moreover, we can see that the robustness of the proposed method is nearly the same as that of MFC method.

Next, we proceeded with experiments using actual HDD.

5 Application to Hard Disk Drive(experiment)

In this section, we show the results of experiments where we applied the trajectory by $Q(t)$ mentioned in section 3.3 to 2.5 inch HDD to verify the effectiveness of proposed method.

5.1 Experimental setup

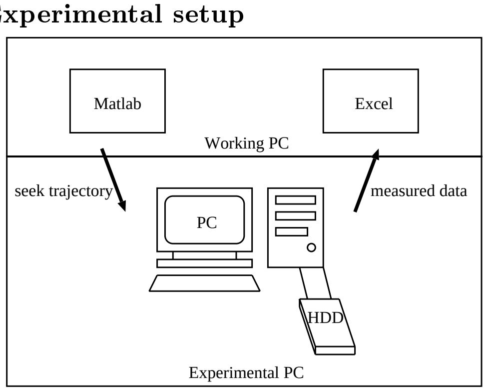

Figure 11: Configuration of Experimental System

Fig.11 shows the configuration of the experimental system.

First, we generated and tabulated the target trajectory of the proposed method on working PC using MATLAB. Next, we used the tabulated data as a feedforward input to actuate the VCM of the 2.5 inch HDD on the experimental PC.

The conventional feedback controller is composed of a PID controller which is already tuned. The feedback system has a sampling time of 132 [μs], but the feedforwad controller has a sampling time of 66 [μs].

In this experiments, we used two different HDDs of HDD♯1 and HDD♯2 in order to test the robustness the proposed method.

5.2 Experimental results

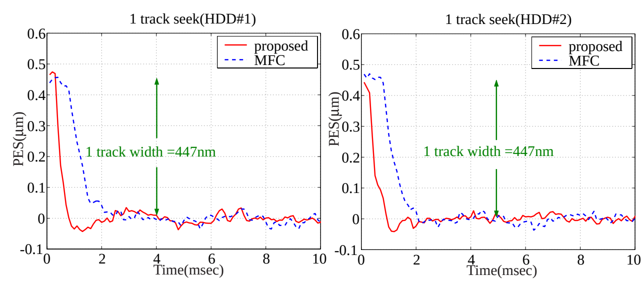

(a) HDD♯1 (b) HDD♯2

Figure 12: 1 track seek (experiment)

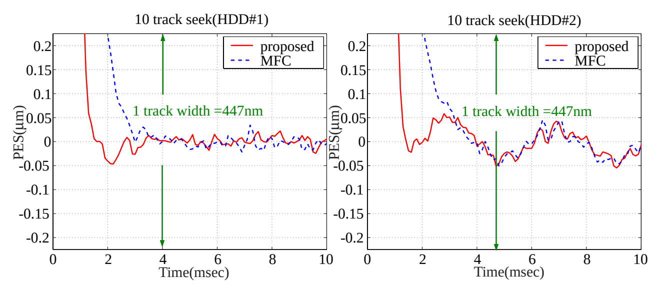

(a) HDD♯1 (b) HDD♯2

Figure 13: 10 track seek (experiment)

Fig.12∼14 show experimental results of the proposed method compared to the MFC trajectory.

From Fig.12∼14, we can see that the head positioning times of 1 track, 10 tracks and 100 tracks are shortened by approximately 50%,50% and 25%, respectively.

Here, the head positioning time is defined by the time taken before the head is positioned within ±10% of one track width.

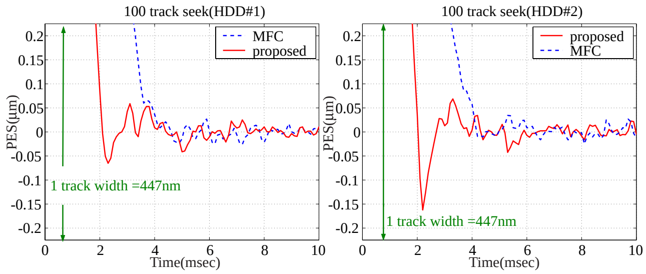

(a) HDD♯1 (b) HDD♯2

Figure 14: 100 track seek (experiment)

6 Conclusion

In this paper, a novel method to design the target trajectory considering the derivative of jerk is proposed, which plays an important role especially in the TDOF control system used for HDD positioning control. The designed smooth trajectory suppresses (or does not activate) mechanical vibration. The trajectory can be modified easily by the choice of weighting functions for further improvement while keeping the initial and terminal conditions strictly. It is experimentally verified that the proposed method is effective in suppressing mechanical vibration and shortening access time.

7 Acknowledgement

The authors would like to acknowledge TOSHIBA Co. Ltd. for supporting and providing the experimental equipments used in this work, and H. Suzuki, S. Yanagihara, M. Yatsu, M. Iwashiro and H. Sado of TOSHIBA Co. Ltd. for their useful discussion and help with the experimental setup.

References

[1] G.E.Franklin,J.D.Powell and M.L.Workman : “Digital Control of Dynamics Systems(3rd edition)”, Addison-Wesley, 1998.

[2] T. Yamaguchi, H. Numasato : “A mode switching control for motion control and its application to disk drives : Design of optimal mode switching conditions”, IEEE/ ASME Trans. on mechatronics, Vol. 3, NO. 3, pp. 202-209, 1998.

[3] J. Ishikawa, T. Hattori, M. Hashimoto : “High-Speed Positioning Control for Hard Disk Drives Based on Two-Degree-of-Freedom Control”, Jour. JSME, Vol.62, No.597-C, pp. 1848-1856, 1996.(in Japanese)

[4] L. Yi, M. Tomizuka : “Two-degree-of-freedom control with robust feedback control for Hard disk servo systems”, IEEE/ASME Trans. on mechatronics, Vol. 4, NO. 1, pp. 17-24, 1999.

[5] Y.Hori and K.Ohnishi : “Applications of Control Engineering”, pp. 36-49, Maruzen, 1998. (in Japanese)

[6] Y. Mizoshita, S. Hasegawa, and K. Takaishi : “Vibration Minimized Access Control for Disk Drives”, IEEE Trans. on Magnetics, Vol. 32, No. 3, pp. 1793-1798, 1996.

[7] S. Hasegawa, K. Takaishi and Y.Mizoshita : “Digital Servo Control for Head-positioning of Disk Drives, Fujitsu Scientific and Technical Journal 26 : (4), pp. 378-390, 1990.

[8] M. Yatsu, H. Suzuki : “Seek Control Method of Hard Disk Drives Using Model Following Control”,74th ordinary general meeting(4), JSME, pp. 410-411, 1997.(in Japanese)

[9] O.V.Beldiman and H.O.Wang : “Trajectory Generation of High-Rise/High-Speed Elevators”, Proceedings of the American Control Conference, pp. 3455-3459. Philadelphia, Pennsylvania, June 1998.

[10] E.V.COOPER : “Minimizing Power Dissipation in a Disk File Actuator” : IEEE Trans. on Magnetics, Vol. 24, NO. 3, pp. 2081-2091, MAY 1988.